Available online at www.sciencedirect.com
SCIENCE DIRECT®
Experimental Eye Research 78 (2004) 137–150
EXPERIMENTAL EYE RESEARCH
www.elsevier.com/locate/yexer

Functional and structural reversibility of H-7 effects on the conventional aqueous outflow pathway in monkeys☆

Ilana Sabanay[a], Baohe Tian[b], B'ann T. Gabelt[b], Benjamin Geiger[a], Paul L. Kaufman[b,*]

[a]*Department of Molecular Cell Biology, Weizmann Institute of Science, Rehovot, Israel*
[b]*Department of Ophthalmology and Visual Sciences, Clinical Science Center, University of Wisconsin, F4/328 CSC-3220, 600 Highland Avenue, Madison, WI 53792-3284, USA*

Received 26 March 2003; accepted in revised form 10 September 2003

Abstract

To determine the mechanism of H-7-induced outflow resistance decrease, the reversibility of H-7 effects on outflow pathway was studied physiologically and morphologically in live monkey eyes. Total outflow facility was measured by two-level constant pressure perfusion before (baseline measurement) and after (post-drug measurement) anterior chamber (AC) exchange with 300 μM H-7 or vehicle in opposite eyes of eight monkeys. H-7 was then removed by AC exchange with drug-free vehicle in both eyes, followed by a 2·5 hr waiting period, after which outflow facility was measured again with (Group 2; $n = 4$) or without (Group 1; $n = 4$) another preceding drug-free AC exchange. For morphological study, five monkeys were initially perfused similarly to Group 1 in physiology, but the facility measurement beginning 2·5 hr after drug removal was either omitted or replaced by gold solution infusion. Following baseline measurement, two of the five monkeys received H-7 or vehicle in opposite eyes, while three monkeys received H-7 in both eyes 2·5 hr apart, contributing one H-7-treated 'recovery' eye and one H-7-treated 'acute' eye. After perfusion, both eyes of all five monkeys were studied by light and electron microscopy. Outflow facility during post-drug measurement in the H-7-treated eye was significantly increased by two-fold. However, the facility increase was reduced when measured beginning 2·5 hr after drug removal, with the reduction being greater in Group 1. 'Recovered' outflow facility after drug removal gradually increased again under continuous AC infusion with drug-free vehicle. Morphologically, major changes in and around Schlemm's canal (SC) in the H-7-treated 'acute' eye included protrusion of the entire inner wall (IW) into SC, relaxation of the IW cells and reorganization of the IW cytoskeleton. The changes in IW cells and juxtacanalicular region of the H-7-treated 'recovery' eye were non-uniform, with areas resembling the vehicle-treated eye ('contracted areas') and areas resembling the H-7-treated 'acute' eye ('relaxed areas'). The average junction-to-junction distances in the IW cells of the H-7-treated 'recovery' eye were intermediate between the vehicle-treated eye and the H-7-treated 'acute' eye. In conclusion, H-7's effect on outflow facility seems reversible, but AC exchange or continuous infusion with drug-free vehicle can re-elevate the 'recovered' outflow facility. Major morphological changes in the TM immediately after H-7 include IW protrusion, cellular relaxation and cytoskeleton reorganization. The decrease in 'relaxed areas' in the TM, in conjunction with the reversed outflow facility, 2·5 hr after drug removal suggests that cellular relaxation in the TM is the structural basis for H-7-induced increase in outflow facility.

Keywords: cytoskeleton; H-7; monkey eye; outflow facility; trabecular meshwork

1. Introduction

The serine-threonine kinase inhibitor H-7 (1-(5-isoquinolinyl-sulfonyl)-2 methylpiperazine) inhibits actomyosin-driven contractility, probably by inhibiting myosin light chain kinase or Rho kinase. This leads to deterioration of the actin microfilament system and perturbation of its membrane anchorage, and loss of stress fibres and focal contacts in many types of cultured cells including human trabecular cells (Birrell et al., 1989; Yu and Gotlieb, 1992; Volberg et al., 1994; Bershadsky et al., 1996; Gills et al., 1998; Tian et al., 1998; Liu et al., 2001). H-7 administered intracamerally or topically to living cynomolgus monkey eyes increases outflow facility and decreases intraocular pressure (IOP) (Tian et al., 1998) by a mechanism independent of the ciliary muscle, presumably acting directly on the trabecular

☆ The University of Wisconsin and the Weizmann Institute of Science hold a patent related to this manuscript; accordingly, Drs Kaufman (UW) and Geiger (WIS) have a proprietary interest.

* Corresponding author. Dr Paul L. Kaufman, Department of Ophthalmology and Visual Sciences, Clinical Science Center, University of Wisconsin, F4/328 CSC-3220, 600 Highland Avenue, Madison, WI 53792-3284, USA.
E-mail address: kaufmanp@mhub.ophth.wisc.edu (P.L. Kaufman).

0014-4835/$ - see front matter © 2004 Elsevier Ltd. All rights reserved.
DOI:10.1016/j.exer.2003.09.007

meshwork (TM) (Tian et al., 1999). The H-7-induced increase in outflow facility is dose-, time- and pressure-dependent (Tian et al., 1998). Although a small portion of the effect of H-7 on outflow facility appears to last several weeks, the major facility increase following H-7 seems reversible 2–3 hr after drug removal from the anterior chamber (AC). However, the 'recovered' facility again becomes gradually elevated by continuous AC infusion with drug-free vehicle (Tian et al., 1998). Morphological study of the TM in the live monkey eye indicates that H-7 induces apparent distension of the juxtacanalicular (JXT) and Schlemm's canal (SC) areas and substantial increase of intercellular spaces, accompanied by a dramatic reduction in intercellular contacts between JXT cells. The tight organization of the cytoskeleton is perturbed, the IW cells generally adopt a flatter, wider 'relaxed' appearance after H-7, and intracamerallly infused gold tracer is distributed much more broadly and uniformly in the JXT and subcanalicular areas (Sabanay et al., 2000). Although it is commonly accepted that the increase in outflow facility after H-7 is related to the structural changes in the TM, mechanisms for the reversibility and re-elevation of outflow facility after H-7's removal are still unknown. However, it seems important to identify what morphological changes in the TM are the structural basis for the functional reversibility in such 'recovered' eyes, since it would help to further understand the mechanism of H-7 effects on resistance in the TM, which might facilitate the development of specific target-selective cytoskeletal anti-glaucoma medications. We therefore specifically studied the functional and structural reversibility of the H-7-induced outflow facility increase and the effect of fluid flow through the TM on the reversibility.

2. Materials and methods

2.1. Animals and anaesthesia

Thirteen normal cynomolgus monkeys (*Macaca fascicularis*), weighing 3–5 kg, were studied, eight in physiology protocols and five in morphology protocols. Most monkeys had undergone prior AC perfusions but not within the preceding 5–6 weeks; all were free of AC cells and flare by slit-lamp biomicroscopy. All investigations were in accordance with University of Wisconsin and NIH guidelines, and with the ARVO Statement on the use of animals in Ophthalmic and Vision Research. Anesthesia was induced by intramuscular (i.m.) ketamine (10 mg kg^{-1}), followed by i.v. (15 mg kg^{-1}) or i.m. (35 mg kg^{-1}) pentobarbital-Na.

2.2. Chemicals and drug preparation

H-7 (1-(5-isoquinolinyl-sulfonyl)-2-methylpiperazine) was obtained from Sigma (St Louis, MO, USA) and stored at 4°C. H-7 solution (300 μM) for perfusions was freshly prepared in Bárány's solution (Bárány, 1964). Cationic colloidal gold (5 nm particles; 5×10^{13} particles ml^{-1} in 20% glycerol) and bovine serum albumin (BSA)-conjugated gold (10 nm particles; $5{\cdot}7 \times 10^{12}$ particles ml^{-1} in 20% glycerol + 1% BSA; optical density = 3·13 at 520 nm) were from British BioCell International Ltd, distributed by Ted Pella, Inc, Redding, CA, USA. BSA-conjugated gold (~4 ml) was dialyzed before use against 300 ml × 3 changes of Bárány's solution. Vehicle + gold solution was formulated as 4·26 ml Bárány's + 240 μl cationized gold (5 nm particles) + 3·50 ml dialyzed non-cationized gold albumin (10 nm particles; optical density = 1·9) or 6·46 ml Bárány's + 240 μl cationized gold (5 nm particles) + 3·30 ml dialyzed non-cationized gold albumin (10 nm particles; optical density = 2·0), so that the final solution contained equal concentrations of 5 nm particles of cationized gold and 10 nm particles of non-cationized gold conjugated to albumin.

2.3. Outflow facility

Total outflow facility was determined by two-level constant pressure perfusion of the AC with Bárány's mock aqueous humour, correcting for the internal resistance of the perfusion apparatus as appropriate (Bárány, 1965). In the physiology protocols, the perfusion pressures were ~15/25mmHg as in previous physiology studies (Tian et al., 1998). In the morphology protocols, the pressures were ~25/35mmHg in both eyes to facilitate flow of gold particles and fixative into the TM. The AC of both eyes of the monkey was cannulated with a branched needle with one branch connected to a reservoir and the other to a pressure transducer, and an unbranched needle with tubing clamped off. Following 35 min baseline facility measurement bilaterally, the clamped tubing from the unbranched needle was then connected to a syringe containing H-7 or vehicle. The syringe was placed in a variable speed infusion pump and the tubing previously connecting one branch of the branched needle to the reservoir was disconnected and opened to air as a temporary outflow line. This allowed infusion of 2 ml of solution through the AC over ~12 min to exchange the AC contents. IOP was maintained at ~15mmHg during the exchange infusion. The reservoir was emptied and re-filled with the same solution being perfused through the eye. After the AC exchange, the 'temporary outflow' tubing was reconnected to the reservoir and the syringe tubing was clamped again, so that the system was ready to continue the facility measurement.

Physiology protocols. To determine the reversibility of H-7 effects on outflow facility and the effect of fluid flow on the reversibility, eight monkeys were studied in these protocols. Following baseline facility measurement, post-drug and post-vehicle outflow facility was determined for 55 min (post-drug measurement) beginning 30 min after AC exchange with 300 μM H-7/vehicle, followed by continuous infusion of H-7 or vehicle from the reservoir to the AC, in opposite eyes. H-7 was then removed by AC exchange with

drug-free Bárány's solution in both eyes, after which the reservoirs were emptied and refilled with drug-free vehicle and closed for 2·5 hr. Outflow facility was then measured again (measurement beginning 2·5 hr after drug removal) with (Group 2; $n = 4$) or without (Group 1; $n = 4$) another preceding AC exchange with drug-free Bárány's solution in both eyes (Fig. 1). All eight monkeys are apparent H-7 responders (with outflow facility in post-drug measurement increased by 50% or more after adjustment for baseline and contralateral control eye washout).

Morphology protocols. To determine the structural basis for the reversibility of H-7 effects on outflow facility by light/electron microscopy (LM/EM), five monkeys were initially perfused as in Group 1/physiology. Following baseline measurement, two monkeys received H-7 or vehicle in opposite eyes, each contributing one H-7-treated 'recovery' eye and one vehicle-treated 'recovery' eye. However, the outflow facility measurement by two-level constant pressure perfusion (25/35mmHg) beginning 2·5 hr after drug removal was replaced by outflow rate measurement at 25mmHg, during which Bárány's + gold solution containing 30 μl ml^{-1} cationic gold (5 nm particles) and 438 μl ml^{-1} dialyzed non-cationized gold albumin (10 nm particles) was allowed to flow into both eyes for 30 or 50 min. Following the gold infusion, the inflow tubing was switched to reservoirs containing Ito's fixative that was allowed to flow into the eyes for 60–90 min at 25mmHg (Fig. 2(A)). In the other three monkeys, baseline outflow facility was measured bilaterally as in the two monkeys above, after which the AC of one eye (the H-7-treated 'recovery eye') for each monkey was exchanged with H-7 immediately (H-7 solution contained gold for one animal), and then post-drug outflow facility of this eye was measured for 45 min beginning 30 min after the AC exchange. The drug was then removed from the AC by an additional AC exchange with drug-free Bárány's solution and the reservoir for this eye was then shut down for 2·5 hr. Following baseline facility measurement, the reservoir for the other eye (the H-7-treated 'acute eye') was closed until 1 hr after the reservoir for the H-7-treated 'recovery eye' had been shut down. Then, the same procedures as for the 'recovery eye' were repeated for the 'acute eye' of each monkey, so that the drug-free AC exchange for the 'acute eye' was finished at the same time as the 2·5 hr recovery period for the 'recovery eye' ended. At this time, both eyes of two of the three monkeys were immediately fixed simultaneously with Ito's fixative for 90 min (Fig. 2(B)). The eyes of the third monkey were fixed with Ito's following a preceding 30-min infusion with drug-free Bárány's + gold solution containing 24 μl ml^{-1} cationic gold (5 nm particles) and 330 μl ml^{-1} dialyzed non-cationized gold albumin (10 nm particles) (Fig. 2(C)).

Before perfusions, the femoral artery and vein of each monkey in the morphology protocols were cannulated. During fixation with Ito's solution (beginning 40–45 min after Ito's flow into the eye), exsanguinations were conducted by infusing lactated Ringers solution through the femoral vein while letting blood flow out of the femoral artery. Blood pressure in the artery during exsanguinations was monitored and maintained at the original level by adjusting the flow of lactated Ringers solution.

2.4. LM and EM of the TM

After fixation, both eyes of the five monkeys in the morphology protocols were enucleated under supplemental pentobarbital anaesthesia just before euthanization by pentobarbital overdose. The anterior segment was quadrisected and placed in Ito's fixative and embedded in Epon-812 (SPI-PON; SPI, West Chester, PA, USA). Specimens

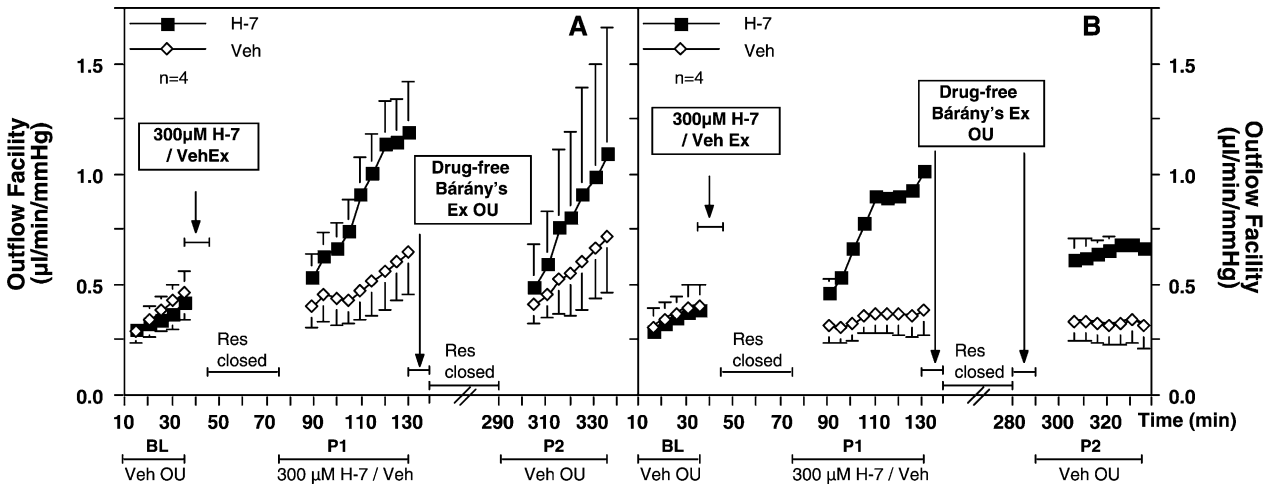

Fig. 1. Effect of fluid flow on reversibility of H-7 effects on outflow facility in monkeys. BL, baseline measurement (35 min); P1, post-drug measurement (55 min); P2, measurement beginning 2·5 hr after drug removal (45 min); Ex, AC exchange; Res, reservoir. An additional AC exchange with drug-free Bárány's solution immediately before P2 was conducted in B (Group 2), but not in A (Group 1). Data are mean ± S.E.M. (l min^{-1} $mmHg^{-1}$ for n animals, each contributing one H-7- and one vehicle-treated eye.

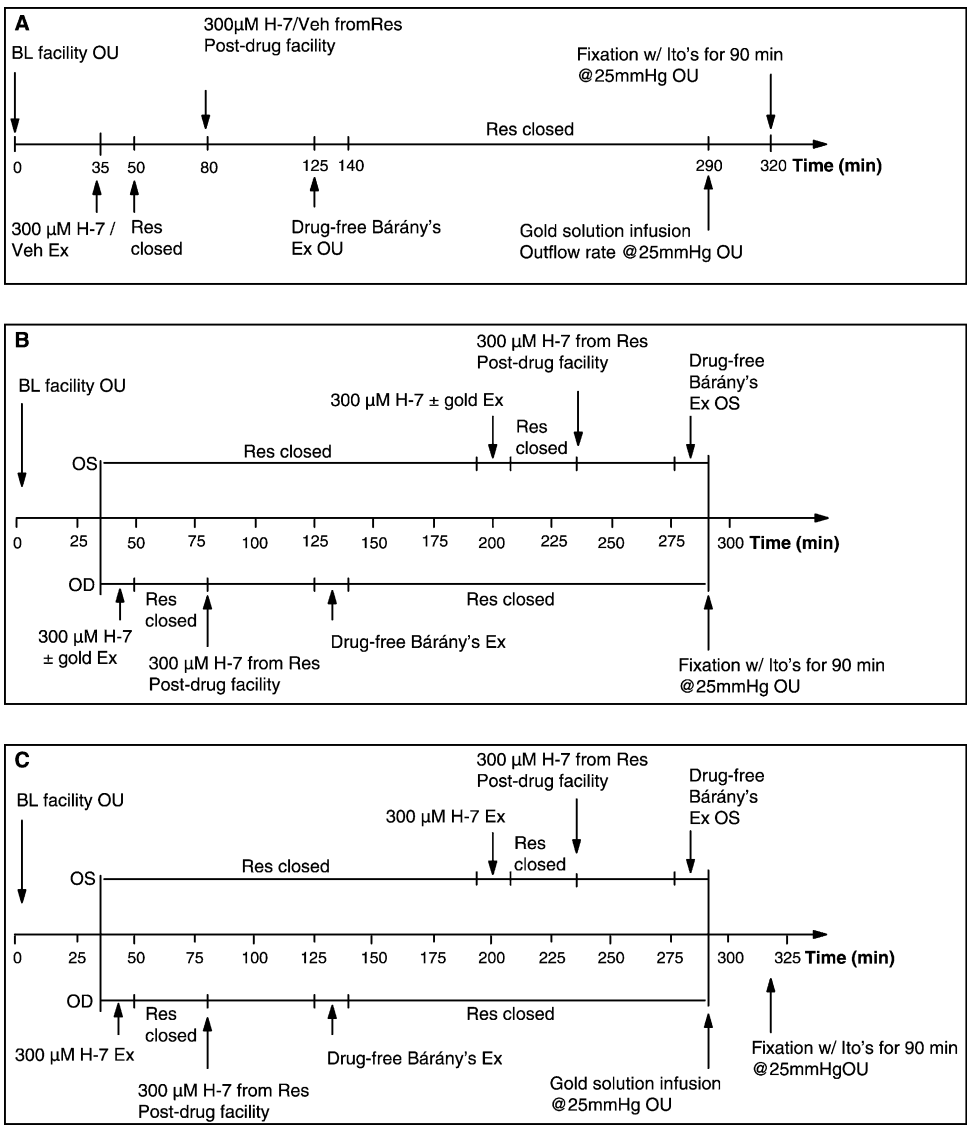

Fig. 2. Time tracks for morphology protocols. BL, baseline measurement (35 min); Ex, AC exchange; Res, reservoir; OU, both eyes; OD, H-7 'recovery' eye; OS, H-7 'acute' eye; Veh, vehicle.

for LM were sectioned (2 μm) with an ultramicrotome (Leica Ultracut-UCT, Vienna, Austria), stained with Epoxy tissue stain (EMS, Fort Washington, PA), and recorded using a digital camera (Nikon E800, DXM1200, Tokyo, Japan). All four quadrants in all eyes were evaluated by LM. Only regions that were grossly intact were examined by EM, usually 2–3 quadrants per specimen. For transmission EM, 700 Å sections were cut in the ultramicrotome, stained with uranyl acetate and lead citrate, examined with a transmission electron microscope (model CM12; Philips, Eindhoven, The Netherlands) and recorded with a SIS Biocam CCD, 1024 × 1024 pixel camera (Münster, Germany). Measurement of junction-to-junction (J–J) distances of the IW cells was performed using the analysis software (Soft Imaging System GmbH, Müenster, Germany), directly on the microscope images. All adherens junctions were marked manually, and the distance between marks was used for calculating cell sizes. The quantitative data of J–J distance of each eye were obtained from ~120 ultrathin sections cut along different regions that were very well preserved and had excellent contrast on the images. Other regions were also examined, but not measured (>10 grids for every specimen, in different quarters).

2.5. Statistical analysis

For the physiology protocols, data are presented as mean ± S.E.M. for *n* eyes or animals. Pre- or post-drug treated vs. contralateral control; post-drug or post-vehicle vs. ipsilateral baseline; and baseline corrected post-drug treated vs. control comparisons were made using the two-tailed paired *t*-test for ratios vs. 1·0 or differences vs. 0·0. Physiology data from morphology protocols are presented per animal.

3. Results

3.1. Outflow facility/outflow rate

Physiology protocols. After adjustment for baselines and resistance washout in the contralateral control eye, post-drug or post-drug-removal outflow facility in the H-7-treated eye was increased by 119 ± 40% ($n = 4$; $P < 0.05$) or 44 ± 44% ($P > 0.3$) in Group 1 that did not receive an additional drug-free AC exchange immediately before the measurement beginning 2·5 hr after drug removal. The last post-drug facility value in the H-7-treated eye was 0·55 ± 0·15 μl min^{-1} mmHg^{-1} (mean ± S.E.M; $P < 0.05$) higher than that in the contralateral control eye. However, the difference declined to 0·08 ± 0·18 μl min^{-1} mmHg^{-1} at the first facility measurement beginning 2·5 hr after drug removal, followed by a gradual increase over time due to a faster facility increase in the H-7-treated eye than that in the contralateral control eye (Fig. 1(A); Table 1(A)). In Group 2 that received an additional drug-free AC exchange immediately before the measurement beginning 2·5 hr after drug removal, post-drug or post-drug-removal outflow facility in the H-7-treated eye was increased by 159 ± 51% ($n = 4$; $P = 0.05$) or 119 ± 19% ($P < 0.01$). The last post-drug facility value in the H-7-treated eye was 0·63 ± 0·09 μl min^{-1} mmHg^{-1} ($P < 0.01$) higher than that in the contralateral control eye. However, the difference was still 0·28 ± 0·07 μl min^{-1} mmHg^{-1} ($P < 0.05$) at the first facility measurement beginning at 2·5 hr after drug removal, and then increased only slightly over time in the H-7-treated eye, probably because the resistance washout reached plateau quickly after the drug-free AC exchange (Fig. 1(B); Table 1B). Additionally, outflow facility in the contralateral control eye in the first four monkeys increased from 0·40 ± 0·10 to 0·64 ± 0·19 μl min^{-1} mmHg^{-1} during post-drug measurement (resistance washout) and then returned to 0·41 ± 0·09 μl min^{-1} mmHg^{-1} at the first facility measurement beginning 2·5 hr after drug removal (reversibility of resistance washout), followed by a gradual increase over time (resistance washout again). The resistance washout and its reversibility in the contralateral control eye in the second four monkeys were similar to but not as great as in the first four monkeys (from 0·32 ± 0·08 to 0·39 ± 0·12 μl min^{-1} mmHg^{-1} in the post-drug measurement and then to 0·34 ± 0·09 μl min^{-1} mmHg^{-1} at the beginning of the measurement after drug removal). Resistance washout in the measurement beginning 2·5 hr after drug removal did not occur in the second four animals. (Table 1; Fig. 1).

Morphology protocols. In the two monkeys that received H-7 or vehicle in opposite eyes, baseline outflow rate was similar in both eyes, but post-drug outflow rate in the H-7-treated eye was substantially higher than that in the contralateral control eye. However, outflow rate in the H-7-treated eye during the measurement beginning 2·5 hr after

Table 1
Effect of AC exchange on the reversibility of H-7 effects on outflow facility

	H-7	Vehicle	H-7/vehicle	H-7 − vehicle
A ($n = 4$)				
Overall 35(BL) or 45 (Rx) min perfusion				
BL	0·35 ± 0·06	0·38 ± 0·06	0·94 ± 0·17	
Rx_{P1}	0·88 ± 0·15	0·50 ± 0·14	2·14 ± 0·70	
Rx_{P2}	0·81 ± 0·39	0·56 ± 0·18	1·49 ± 0·67	
Rx_{P1}/BL	2·53 ± 0·22	1·23 ± 0·18	2·19 ± 0·40Y	
Rx_{P2}/BL	2·28 ± 1·03	1·42 ± 0·31	1·44 ± 0·44	
Specific single values				
$P1_{1st}$	0·53 ± 0·11	0·40 ± 0·10		0·13 ± 0·11
$P1_{last}$	1·19 ± 0·23	0·64 ± 0·19		0·55 ± 0·15†
$P2_{1st}$	0·49 ± 0·19	0·41 ± 0·09		0·08 ± 0·18
B ($n = 4$)				
Overall 35(BL) or 45 (Rx) min perfusion				
BL	0·35 ± 0·04	0·36 ± 0·09	1·14 ± 0·27	
Rx_{P1}	0·79 ± 0·02	0·35 ± 0·08	2·96 ± 1·07	
Rx_{P2}	0·65 ± 0·05	0·33 ± 0·09	2·38 ± 0·46	
Rx_{P1}/BL	2·36 ± 0·26	0·97 ± 0·13	2·59 ± 0·51*	
Rx_{P2}/BL	1·96 ± 0·25	0·89 ± 0·05	2·19 ± 0·19‡	
Specific single values				
$P1_{1st}$	0·46 ± 0·06	0·32 ± 0·08		0·15 ± 0·11
$P1_{last}$	1·02 ± 0·03	0·39 ± 0·12		0·63 ± 0·09‡
$P2_{1st}$	0·62 ± 0·10	0·34 ± 0·09		0·28 ± 0·07†

Effect of AC exchange with drug-free vehicle on the reversibility of 300 μM H-7 effects on outflow facility in living monkeys. A: Monkeys that did not receive an additional preceding drug-free AC exchange before the measurement 2·5 hr after drug removal; B: Monkeys that received an additional drug-free AC exchange before the measurement 2·5 hr after drug removal; BL = baseline; Rx = post-drug; P1 = post-drug measurement; P2 = measurement 2·5 hr after drug removal; Rx_{P1} or Rx_{P2} = post-drug/vehicle outflow facility in P1 or P2; $P1_{1st}$ = first value of P1 outflow facility; $P1_{last}$ = last value of P1 outflow facility; $P2_{1st}$ = first value of P2 outflow facility. Facility data are mean ± S.E.M. (μl min^{-1} mmHg^{-1}) for n animals, each contributing one eye receiving H-7 and one receiving vehicle. Ratios are unitless. $^{*}P = 0.05$,$^{\dagger}P < 0.05$; $^{\ddagger}P < 0.01$ by the two-tailed paired t-test for differences $\neq 0.0$ or ratios $\neq 1.0$.

Table 2
Reversibility of H-7 effects on outflow rate in monkeys

	Monkey in Fig. 3A		Monkey in Fig. 3B	
	H-7	Vehicle	H-7	Vehicle
BL	4·18	6·11	4·39	6·43
P1				
Initial 10 min	29·71	7·09	15·53	6·90
After 10 min	43·74	10·61	30·61	14·30
P2				
Initial 10 min	7·67	6·54	7·96	5·66
After 10 min	17·17	12·54	11·19	7·17

This table shows the reversibility of H-7 effects on outflow rate in the two monkeys that received 300 μM H-7 or vehicle in opposite eyes in the morphology protocol (Fig. 2(A)). Outflow rates (μl min^{-1}) at 25mmHg during baseline measurement (BL) and post-drug measurement (P1) were obtained from the two-level constant pressure perfusion (25/35mmHg). Outflow rate at 2·5 hr after drug removal (P2) was obtained from the measurement during gold solution infusion at 25mmHg following the 2·5 hr waiting period (Fig. 3).

drug removal initially fell to a level similar to that in the contralateral control eye, and then gradually increased again over time (Table 2; Fig. 3). In the three monkeys that received H-7 in both eyes 2·5 hr apart, post-drug facility or outflow rate in all eyes was substantially increased compared to ipsilateral baseline (data not shown). Their facility or outflow rate beginning 2·5 hr after drug removal was not measured.

3.2. Morphology

LM. As shown in Fig. 4, the trabecular segment of the pathway was not grossly affected by the addition of H-7 or its withdrawal. The overall geometry of the pathway was not affected and the collagen beams retained a normal appearance. There were, however, some typical changes in the morphology of the SC. In the H-7-treated 'acute' eye, there was a major protrusion of the IW towards the lumen of the SC, particularly prominent in the central region of the canal, and separation of the IW cells from the underlying JXT cells. In the H-7-treated 'recovery' eye, the IW of SC

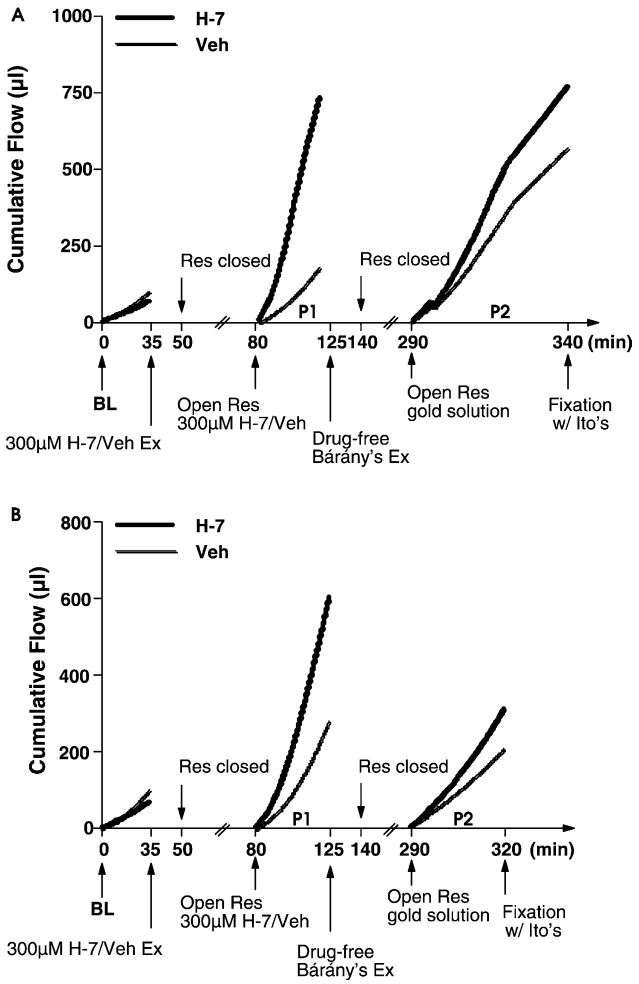

Fig. 3. Cumulative outflow in the two monkeys that received H-7 or vehicle in opposite eyes before fixation ($n = 1$ in panel A and B). BL, baseline measurement (35 min); P1, post-drug measurement (45 min); P2, measurement beginning 2·5 hr after drug removal (50 min in A; 30 min in B); Ex, AC exchange; Res, reservoir. Note that the flow during BL or P1 was obtained from two-level constant pressure perfusion (25/35mmHg), but only the flow at 25mmHg is displayed. The flow in P2 was obtained from the measurement during gold solution infusion at 25mmHg. Calculation of the cumulative flow for each period started from zero.

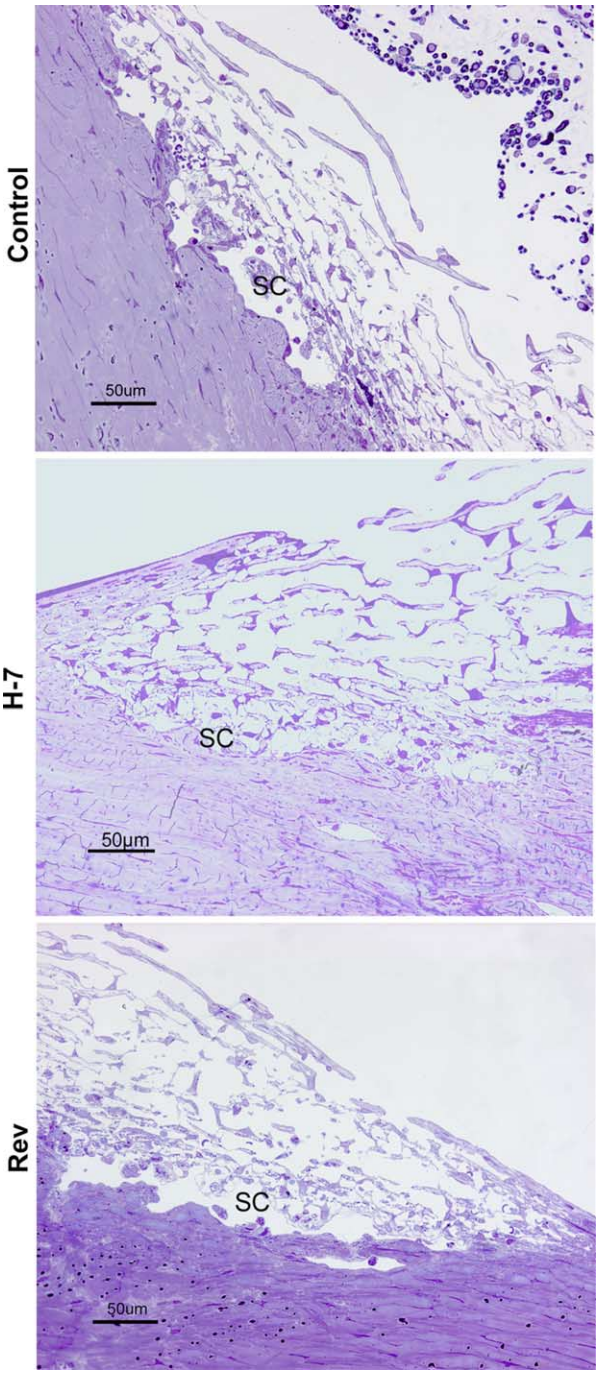

Fig. 4. Low magnification light microscopic view of the trabecular meshwork. H-7, H-7-treated 'acute' eye; Rev, H-7-treated 'recovery' eye; Control, vehicle-treated eye. The trabecular meshwork and Schlemm's canal (SC) remain intact in the H-7-treated 'acute' eye and the H-7-treated 'recovery' eye. In the H-7-treated 'acute' eye, there is a major protrusion of the inner wall toward the lumen of SC. In the H-7-treated 'recovery' eye, the inner wall is highly non-uniform, with alternating protruding and retracted regions.

became highly non-uniform, with alternating protruding and retracted regions (Figs. 4 and 5).

EM. As shown in Figs. 6–9, distribution of gold particles in the outflow pathway differed between vehicle-treated eyes, H-7-treated 'acute' eyes and H-7-treated 'recovery' eyes (see below). However, no observable difference was found in the distribution of cationized and non-cationized gold particles in any eye. Both cationized and non-cationized gold particles tended to bind to the ECM along the outflow pathway. The vehicle-treated eyes exhibited different features of the IW cells, including variable thickness, the occasional presence of giant vacuoles and the presence of ECM along the sub-endothelial region. JXT cells and their processes were abundant along the basal aspects of the IW cells, often directly contacting them (Fig. 6(a)). Higher magnification revealed sparsely distributed gold particles, associated with the sub-IW cells (Fig. 6(b)). Within the cytoplasm, highly ordered arrays of intermediate filaments were noted (Fig. 6(c)). Overall, these features are similar to those previously described (Sabanay et al., 2000). In H-7-treated 'acute' eyes, major morphological changes occurred in the IW cells and JXT region, including protrusion of the entire IW into the SC (Fig. 7(a)), relaxation of the IW cells and reorganization of the IW cytoskeleton (Fig. 7(b)), accompanied by considerable loss of electron-dense ECM from the JXT region, as previously described (Sabanay et al., 2000). Cell–cell junctions were retained and gold particles were abundant throughout the sub-IW space (Fig. 7(b) and (c)). Examination of the same region in H-7-treated 'recovery' eyes revealed a non-uniform morphology along the IW, with regions that largely resembled those of the vehicle-treated eye ('contracted regions', Fig. 8(a)–(c)), alternating with 'relaxed areas' similar to the IW of the H-7-treated 'acute' eye (Fig. 9(a)–(c)). The two areas were usually comparable in extent. The 'contracted areas' were usually retracted from the lumen of SC, and contained well-organized sub-IW spaces with JXT cells bridging between the SC and the TM beams (Fig. 8(a)). Cell–cell junctions were retained and sub-IW ECM was abundant (i.e. re-appearance of ECM deposits), with moderate amounts of associated gold particles. Occasionally, gold-containing vesicles were detected close to the lumenal membrane of the IW cells, suggesting that the gold particles were transported into the canal by transcytosis through the IW cells. The cytoskeletal packing within the cytoplasm also recovered to normal (Fig. 8(b) and (c)). The 'relaxed areas' along the IW in H-7-treated 'recovery' eyes were usually associated with general protrusion into the lumen of the SC, dilation of the sub-IW space and loss of cytoskeletal organization (Fig. 9(a)–(c)). High concentrations of gold

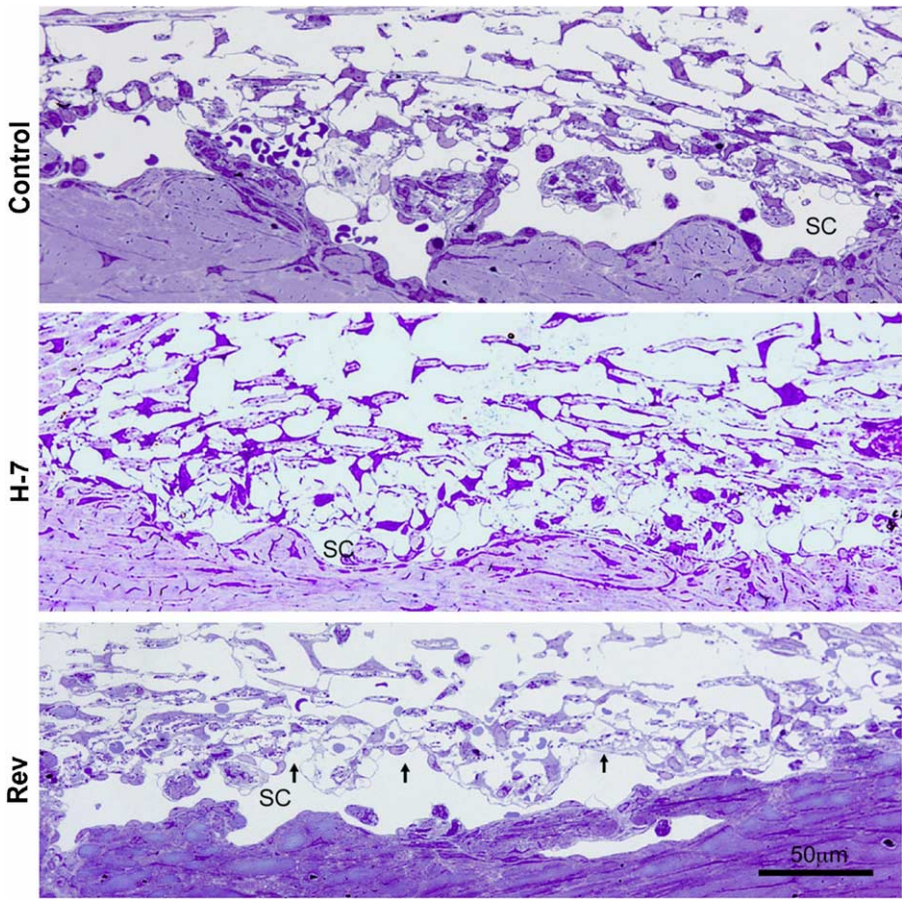

Fig. 5. High magnification of Fig. 4. Arrows indicate the retracted regions in the H-7-treated 'recovery' eye.

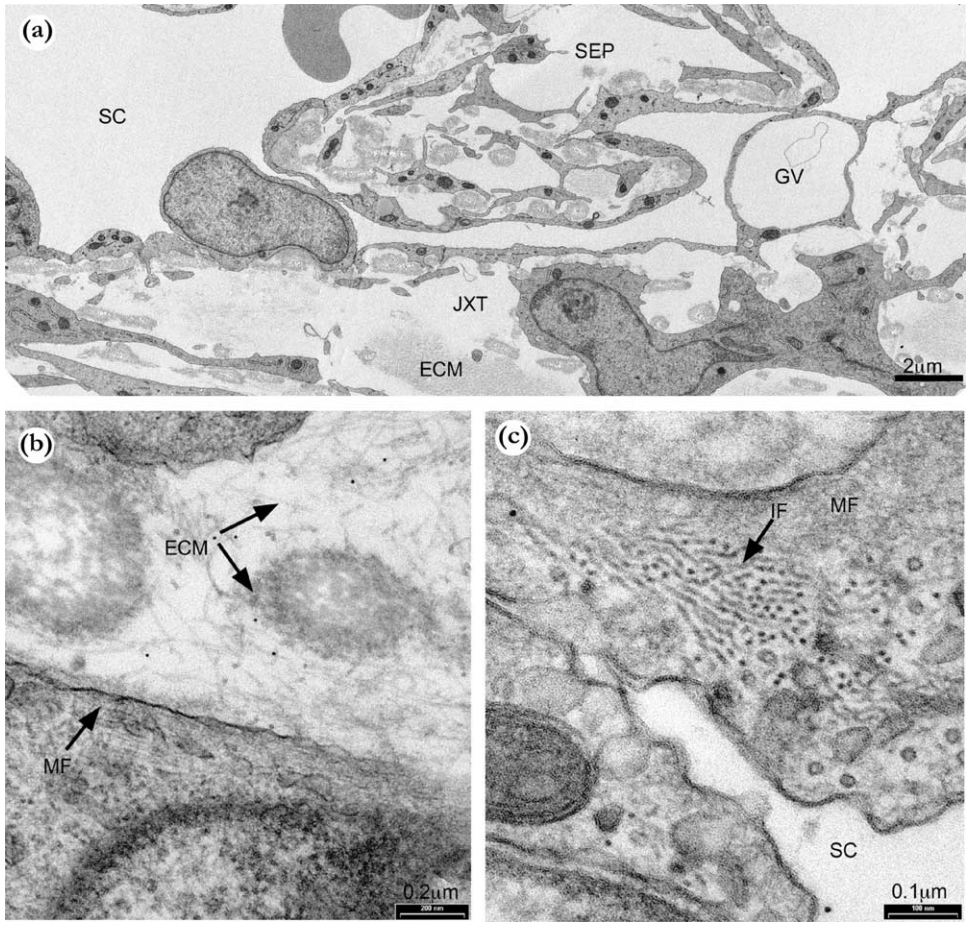

Fig. 6. Electron microscopy of the contralateral control eye (vehicle-treated 'recovery' eye) for the H-7 'recovery' eye (see Figs. 8 and 9). (a) Low magnification view of the Schlemm's canal (SC) and juxtacanalicular (JXT) regions shows a septal structure (SEP) in the lumen of the canal, the presence of extracellular material (ECM) in the JXT region and the presence of giant vacuoles (GV) in the inner wall cells. (b) Higher power magnification of the JXT region shows scattered gold particles (small black dots) associated with a loose array of subcanalicular fibers (arrows). MF, microfilaments (arrow). (c) High power magnification image shows tightly packed arrays of intermediate filaments (IF) in the inner wall endothelial cells (arrow).

particles were present in these areas, associated with residual ECM (Fig. 9(b) and (c)). The ECM in the JXT area in the vehicle-treated eye, the H-7-treated 'acute' eye and the H-7-treated 'recovery' eye was commonly organized in discrete collagen-like fibres.

To further characterize the 'regional' organization of the IW after H-7 withdrawal, we measured the J–J distances along the IW in the vehicle-treated eye, the H-7 treated 'acute' eye and the H-7-treated 'recovery' eye (Fig. 10). The measured J–J distances were naturally variable, according to the specific region in each cell included in the section. However, the quantitative data of the vehicle-treated eye, the H-7-treated 'acute' eye or the H-7-treated 'recovery' eye were based on ~120 ultrathin sections cut along different regions of each eye, and were in line with many repetitions in different animals (in total at least 5–7 animals for vehicle and H-7-treated 'acute' eyes from this study and a previous study (Sabanay et al., 2000); two animals for the H-7-treated 'recovery' eye from the present study only), significantly reducing a possible confounding by natural variability in the J–J distance. Comparison of the vehicle-treated eye to the H-7-treated 'acute' eye revealed a doubling of the average cell width, in agreement with previous findings (Fig. 10) (Sabanay et al., 2000). Interestingly, the H-7-treated 'recovery' eye regained a contracted morphology (e.g. cells # 24–40 of one eye in Fig. 10), flanked by relaxed areas (e.g. cells 45–55 of the same eye in Fig. 10). The average J–J distances in the IW of the H-7-treated 'recovery' eye were intermediate (e.g. 3·8 ± 2·7 μm), between the vehicle-treated eye (e.g. 2·8 ± 1·7 μm) and the H-7-treated 'acute' eye (e.g. 7·3 ± 7·2 μm). Although the averaged J–J distance in the IW of the H-7-treated 'recovery' eye varied somewhat in different monkeys or protocols (Fig. 2), the tendency was always the same; i.e. the value in the H-7-treated 'recovery' eye was always much smaller than that in the H-7-treated 'acute' eye, but slightly larger than that in the vehicle-treated eye. Additionally the monkey in Fig. 3(A) had a little bit larger averaged J–J distance in the H-7-treated 'recovery' eye than the monkey in Fig. 3(B) (4 vs. 3·8 μm), in agreement with the former

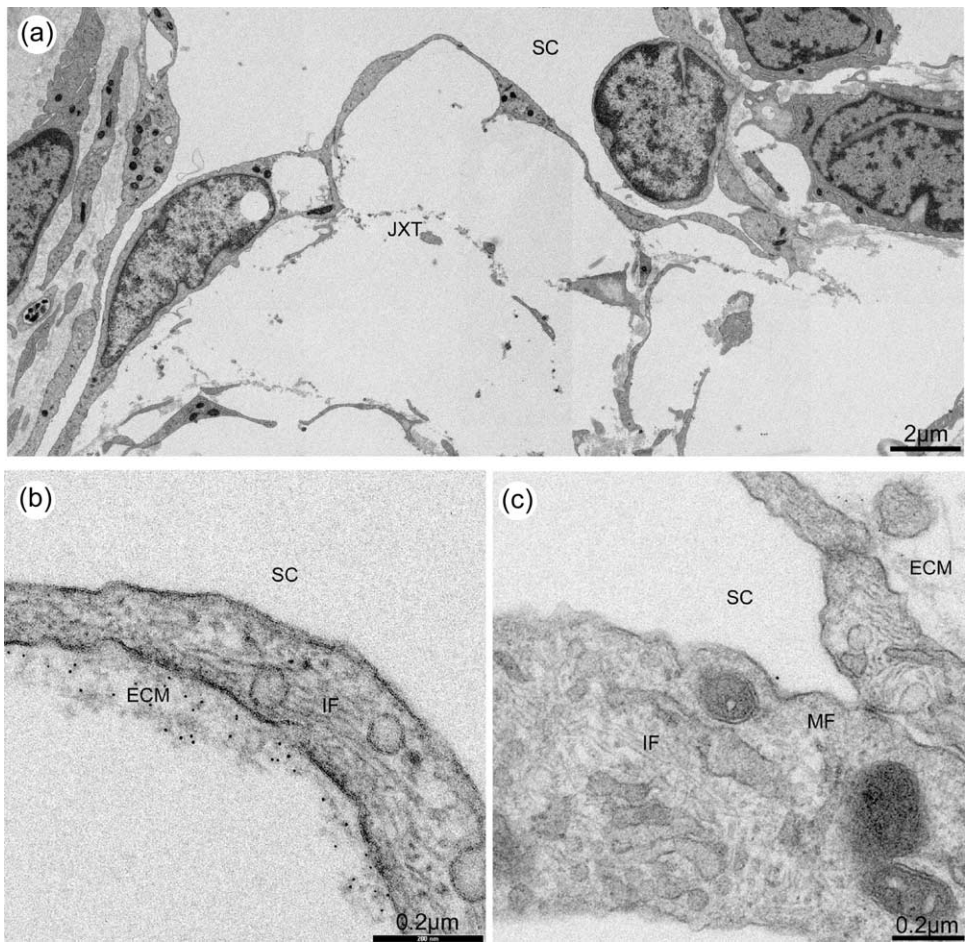

Fig. 7. Electron microscopy of the eye immediately after H-7 (H-7 'acute' eye). (a) Low magnification view of Schlemm's canal (SC) and juxtacanaicular (JXT) regions shows absence of extracellular material (ECM) from the JXT region and presence of 'relaxed' inner wall cells (b) Higher power magnification of the inner wall/JXT region shows gold particles (small black dots) associated with residual ECM, and (c) loose and disorganized arrays of intermediate filaments (IF) and microfilaments (MF) in the IW cells.

having received a longer duration of gold solution infusion (50 vs. 30 min) and exhibiting a greater outflow rate (Table 2; Fig. 3) before fixation than the latter.

4. Discussion

Similar to our previous study (Tian et al., 1998), the modified reversibility protocol in the present study has shown that the H-7-induced increase in outflow facility is reversible after the drug is removed from the AC for 2·5 hr. A continuous infusion of drug-free vehicle is able to re-elevate the 'recovered' outflow facility over time. The AC exchange with drug-free vehicle immediately before the measurement beginning 2·5 hr after drug removal partially inhibits the reversibility or re-elevates the 'recovered' outflow facility quickly. Both findings suggest that the fluid flow through the TM may re-open the 'recovered' outflow pathways. Per previous studies (Mäepea and Bill, 1989, 1992), the pressure in SC (P_{SC}) of the monkey eye is ~7·6–14·3mmHg when spontaneous IOP is ~12·2–19·2mmHg. The relationship between the pressures in the SC and AC is grossly defined as 'IOP = 0·73 P_{SC} + 8·7mmHg'. However, when IOP is increased stepwise from the spontaneous level to 30mmHg, the P_{SC} is only slightly increased by ~1·7mmHg. Therefore, the pressure gradient between the SC and the AC is increased when IOP is increased. IOP during perfusions (15/25mmHg) or AC exchange (~15mmHg) is higher than that during the 2·5-hr recovery period (~7mmHg under pentobarbital anaesthesia (Erickson-Lamy et al., 1984), and fluid flow through the AC driven by the pump during AC exchange produces high-frequency pressure fluctuation (~1mmHg) that may induce flow pulses against the surface of the TM. The mechanism for the re-elevation of outflow facility after the reversibility therefore could be related to the pressure gradient between the AC and SC and/or the pressure fluctuation in the AC.

To determine structural changes in the TM during the reversibility and the re-elevation of outflow facility, we conducted LM/EM studies on monkeys that underwent perfusions similar to those in the physiology protocols, but received a cationized + non-cationized gold solution

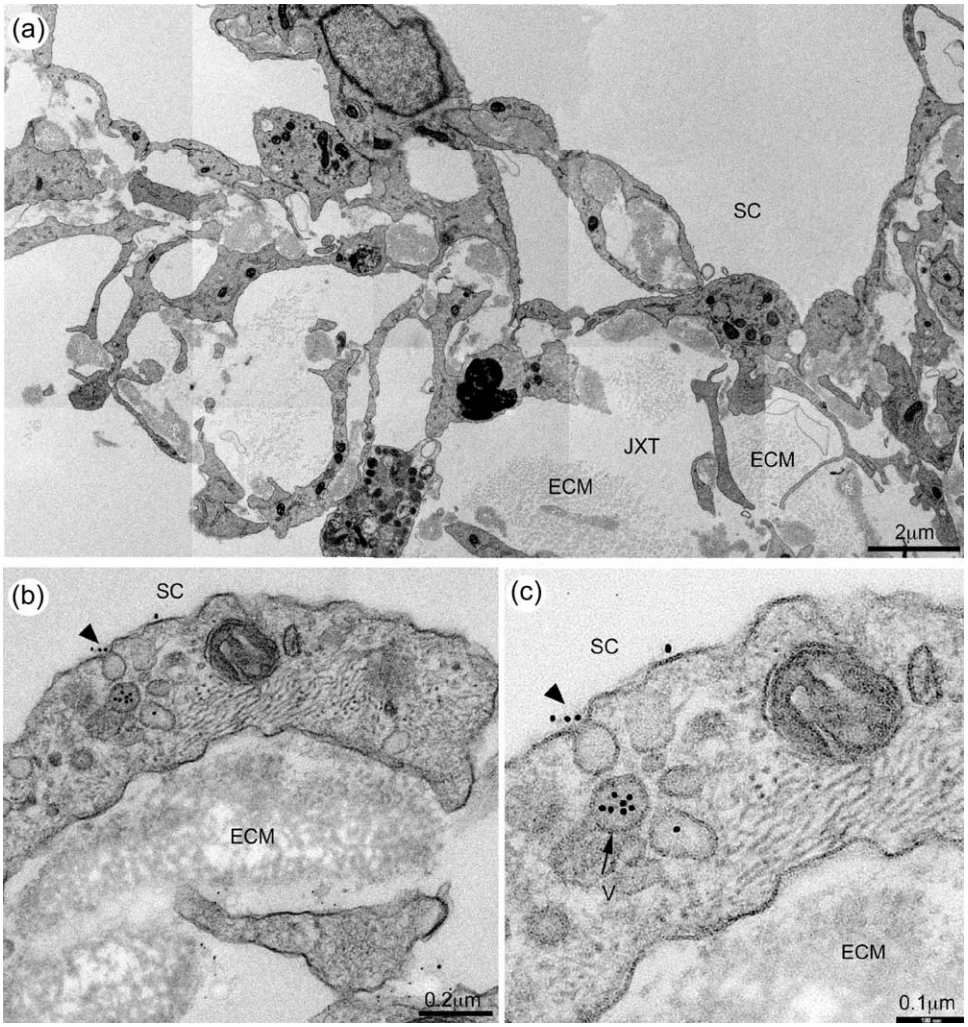

Fig. 8. Electron microscopy of H-7 'recovery' eye—A 'contracted' region along Schlemm's canal (SC). (a) Low magnification view of the SC and juxtacanaicular (JXT) regions shows 're-appearance' of extracellular material (ECM) deposits in the JXT region and presence of 'contracted' inner wall cells. (b) Higher power magnification of the JXT region shows sparse gold particles (small black dots) associated with dense, apparently new ECM deposits. The ECM-bound gold may be undergoing transcytosis, being transported from the basal to the lumenal aspect of the inner wall cells (arrowhead). (c) High power magnification image shows tightly packed arrays of intermediate filaments in the inner wall endothelial cells and gold particles in vesicles (V) throughout inner wall cells (arrow). The arrowhead indicates the transcytosis of gold particles as in (b).

infusion either during the AC exchange or immediately before the fixation in some protocols. To facilitate flow of gold particles and fixative into the TM, the perfusion pressures were also elevated to ~25/35mmHg in both eyes in the morphology protocols. Although the higher pressures (25/35mmHg) may induce a stronger resistance washout and possibly more apparent pressure-dependent changes in the TM after the drug when compared to the lower pressures (15/25mmHg) as in physiology protocols, they will not affect the conclusions based on the difference between eyes that were perfused at the same pressures. Unlike a previous study (Ethier and Chan, 2001), no observable difference was found in the distribution of cationized and non-cationized gold particles in any eye. Both cationized and non-cationized gold particles are not merely 'fluid phase markers' but tend to bind to the ECM along the outflow pathway (Sabanay, et al., 2000), which is of assistance to the comparison in the TM morphology between the H-7-treated 'recovery' eye and the contralateral vehicle-treated eye or the contralateral H-7-treated 'acute' eye.

As described previously (Sabanay et al., 2000), the IW cells in the vehicle-treated eye are in a 'contracted' state with highly ordered arrays of intermediate filaments within the cytoplasm; in the H-7-treated 'acute' eye, major morphological changes in and around SC include protrusion of the entire IW into the SC, relaxation of the IW cells and reorganization of the IW cytoskeleton. The overall protrusion of the IW into the lumen, which seems to indicate that the 'relaxed' IW after H-7 cannot resist the pressure, may account, at least in part, for the increase in the area of the drainage pathway. However, the same region in the H-7-treated 'recovery' eye shows a non-uniform morphology along the IW, with 'contracted' regions similar to those in

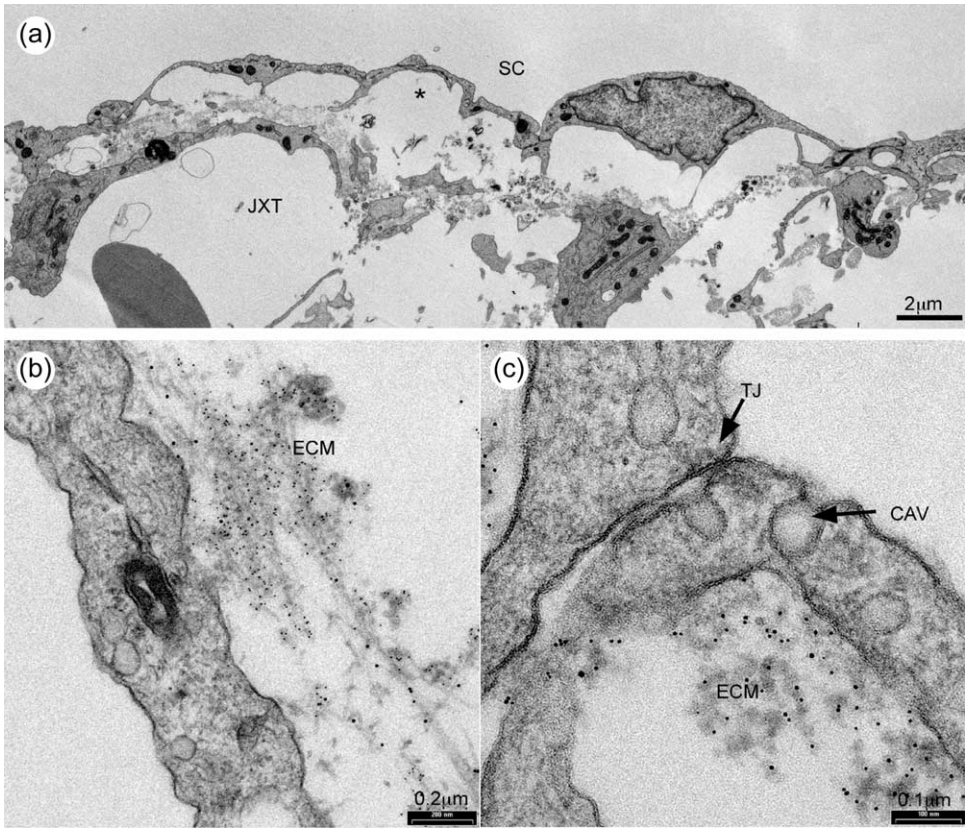

Fig. 9. Electron microscopy of H-7 'recovery' eye—A 'relaxed' region along Schlemm's canal (SC). (a) Low magnification view of the SC and juxtacanalicular (JXT) regions shows absence of extracellular material (ECM) in the JXT region and presence of 'relaxed' inner wall cells (asterisks). (b) Higher power magnification of the JXT region shows many gold particles (small black dots) associated with residual ECM fibers. (c) High power magnification image shows loose and disorganized arrays of intermediate filaments in the inner wall endothelial cells. Tight junctions (TJ) are unaffected. CAV, caveoli.

the vehicle-treated eye and 'relaxed' regions similar to those in the H-7-treated 'acute' eye. Accordingly, the average J–J distance in the IW of the H-7-treated 'recovery' eye is intermediate between the vehicle-treated eye and the H-7-treated 'acute' eye. It is not clear what determines the 'contracted' regions and the 'relaxed' regions in the recovery stage. However, since our physiology data indicate that a continuous infusion of drug-free vehicle or AC exchange with drug-free vehicle immediately before the measurement beginning 2·5 hr after drug removal is able to re-elevate the 'recovered' outflow facility, different flow rates or pressures in different regions in the TM during the recovery period may be responsible for the non-uniform morphology. Additionally, the 'contracted' cells may not necessarily mean that the cells have completely recovered from H-7-induced relaxation. These cells may 'contract' or 'retract' under the lower pressure/fluid flow rate during the 2·5 hr waiting period. However, they may more easily be extended or expanded again under the higher pressure/fluid flow rate after the perfusion is restarted than normal cells, which may explain the progressive re-increase in outflow facility shortly after re-starting perfusion with drug-free Bárány's solution. The still 'relaxed' endothelial cells in the TM of the H-7-treated 'recovery' eye may be related to the effect of fluid flow through the TM during gold infusion immediately before Ito's fixation, but incomplete recovery of H-7-induced cellular relaxation in the TM cannot be excluded. Nevertheless, the re-'contracted' endothelial cells could reduce the area of the drainage surface, and in turn decrease outflow facility.

In the present, as well as previous (Sabanay et al., 2000) study, ECM in the region along the basal aspects of the IW cells of the H-7-treated 'acute' eye was markedly reduced, compared to the vehicle-treated eye. This may indicate either that H-7 increases the ECM washout from the JXT region as previously proposed (Sabanay et al., 2000), or that the IW cells in the H-7-treated 'acute' eye 'balloon' towards the canal, leaving behind the ECM deposits or part of them in more proximal areas of the outflow pathway. However, to date we cannot state whether the ECM that was localized in that region was transported to the SC or 'diluted' in more proximal areas of the outflow pathway. Additionally, this study also revealed some 're-appeared' ECM deposits in the JXT region of the H-7-treated 'recovery' eye. The 're-appeared' ECM in the H-7-treated 'recovery' eye seems much more dense than the ECM in the vehicle-treated eye. However, it is also not clear whether the 're-appearance' of ECM indicates that the ECM 'diluted' in more proximal areas of the outflow pathway by 'ballooned' IW cells re-condenses to its original position when the IW cells

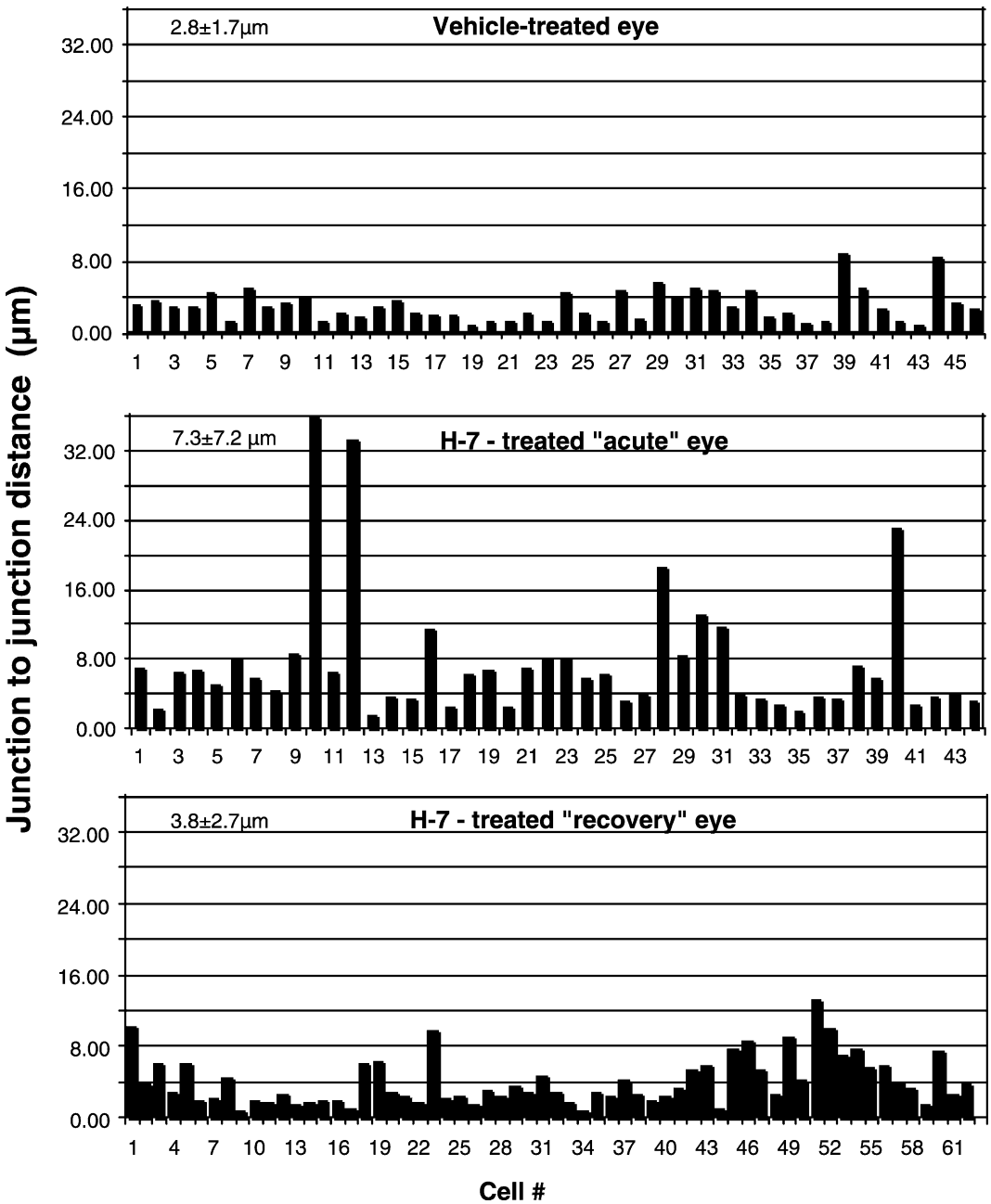

Fig. 10. Histograms show the junction-to-junction distance ((m) in the inner wall of Schlemm's canal. The variability in cell size is partly attributable to the variable orientation of the cells as well as to differences in cell contraction. Data in each panel is obtained from one relevant eye. Note the 'relaxing' effect of H-7, with doubling of the average cell width in the H-7-treated 'acute' eye vs. the vehicle-treated eye, and the presence of 'contracted regions' (e.g. cells #10–40) and 'relaxed regions' (e.g. cells #45–55) along the canal in the H-7-treated 'recovery' eye.

re-contract, or that new biosynthesis of ECM occurs during the 2·5 hr waiting period, or both. Further studies are needed to clarify this issue.

Resistance 'washout' refers to the progressive increase in outflow facility that occurs during prolonged perfusion with drug-free mock aqueous humour in both in vivo and enucleated non-human eyes (Kaufman et al., 1988; Erickson-Lamy et al., 1990). In the present study, we noted that resistance washout in the contralateral vehicle-treated eye was also reversible after the 2·5 hr recovery period. The mechanisms for the reversibility of resistance 'washout' are not clear yet. Since wash-away of ECM from the outflow pathway may be the mechanism of the resistance 'washout' (Johnson et al., 1993; Kee et al., 1996; Gual et al., 1997), a reasonable hypothesis could be that the ECM newly synthesized during the 2·5 hr waiting period may be involved in the reversibility of resistance 'washout'. However, it is unknown if the ECM biosynthesis could occur within 2–3 hr. Additionally, recent studies show that washout may result from a loss of aqueous

funnelling through preferential channels, caused by separation of the IW cells from the underlying JXT connective tissue during perfusion (Johnson et al., 1992; Overby et al., 2002). This suggests that the ECM wash-away mechanism alone may not be sufficient to explain resistance 'washout', and that pressure-induced cellular structural changes from the perfusion may be also involved. Since there are some similar TM structural changes in the perfusion-induced resistance 'washout' and the H-7-induced outflow increase (e.g. ECM washout and separation of the IW cells from the underlying JXT cells), and since the effect of H-7 on outflow facility is pressure-dependent, one might hypothesize that H-7 may simply accelerate the resistance washout process. However, the key structural change for H-7 to increase outflow facility is cellular relaxation, which did not occur during drug-free perfusions.

Taken together, the present data support that the re-'contracted' cells in the TM are the primary structural basis for the reversibility of the H-7-induced increase in outflow facility. This indicates that H-7 effects represent transient alterations in the cellular contractility and cytoskeletal organization rather than irreversible toxicity, important for a potential anti-glaucoma medication since safety is a major consideration. However, the reversibility may also indicate that the effect of H-7 on outflow facility is short-lived, so that H-7, as with all currently available anti-glaucoma medications, may need frequent repetitive administrations to maintain lower IOP. Nevertheless, H-7's effect on outflow facility may last longer in the glaucomatous eye with elevated IOP, since as the IOP returns toward baseline in the glaucomatous eye due to reduced concentration of H-7 in the TM over time, aqueous humour driven by the high pressure gradient between the AC and SC may reopen the 'recovered' outflow pathway, similar to the situation in the facility measurement beginning 2·5 hr after drug removal in the current experiments. Additionally, a single intracameral injection of H-7 in glaucomatous eyes might wash out abnormal ECM and produce long-lasting ocular hypotension, as a so-called one-time 'pharmacologic trabeculocanalotomy' (Kaufman et al., 1979; Epstein, 1987; Kaufman, 1992). Moreover, recent advances in molecular genetics and gene transfer technology (Borrás et al., 1996; Liu et al., 1999; Borrás et al., 2001; Vittitow et al., 2002) may allow long-term re-setting of these outflow regulatory mechanisms to therapeutic advantage in glaucoma. Thus, one can imagine over or under-expressing a particular kinase in the TM cells of the living eye so as to partially inhibit cellular contractility and 'loosen' cell–cell or cell–ECM attachments, thereby permanently increasing outflow facility and reducing IOP.

Acknowledgements

This study was supported by grants from the US National Eye Institute (EY02698), the American Health Assistance Foundation, the Glaucoma Research Foundation, Research to Prevent Blindness, the Wisconsin Alumni Research Foundation, and the Ocular Physiology Research and Education Foundation. B.G. is the incumbent of the E. Neter Chair in Cell and Tumour Biology. The authors thank Jennifer Seeman and Julie Kiland for conducting cannulations of femoral artery and vein in monkeys.

References

Bárány, E.H., 1964. Simultaneous measurement of changing intraocular pressure and outflow facility in the vervet monkey by constant pressure infusion. Invest. Ophthalmol. 3, 135–143.

Bárány, E.H., 1965. Relative importance of autonomic nervous tone and structure as determinants of outflow resistance in normal monkey eyes (*Cercopithecus ethiops* and *Macaca irus*). In: Rohen, J.W. (Ed.), The Structure of the Eye, Second Symposium, F.K. Schattauer, Stuttgart, pp. 223–236.

Bershadsky, A., Chausovsky, A., Becker, E., Lyubimova, A., Geiger, B., 1996. Involvement of microtubules in the control of adhesion-dependent signal transduction. Curr. Biol. 6, 1279–1289.

Birrell, G.B., Hedberg, K.K., Habliston, D.L., Griffith, O.H., 1989. Protein kinase C inhibitor H-7 alters the actin cytoskeleton of cultured cells. J. Cell Physiol. 141, 74–84.

Borrás, T., Gabelt, B.T., Klintworth, G.K., Peterson, J.C., Kaufman, P.L., 2001. Non-invasive observation of repeated adenoviral GFP gene delivery to the anterior segment of the monkey eye in vivo. J. Gene Med. 3, 437–449.

Borrás, T., Tamm, E.R., Zigler, J.S., 1996. Ocular adenovirus gene transfer varies in efficiency and inflammatory response. Invest. Ophthalmol. Vis. Sci. 37, 1282–1293.

Epstein, D.L., 1987. Open angle glaucoma. Why not a cure? Arch. Ophthalmol. 105, 1187–1188.

Erickson-Lamy, K.A., Kaufman, P.L., McDermott, M.L., France, N.K., 1984. Comparative anesthetic effects of aqueous humor dynamics in the cynomolgus monkeys. Arch. Ophthalmol. 102, 1815–1820.

Erickson-Lamy, K., Schroeder, A.M., Bassett-Chu, S., Epstein, D.L., 1990. Absence of time-dependent facility increase (washout) in the perfused enucleated human eye. Invest. Ophthalmol. Vis. Sci. 31, 2384–2388.

Ethier, C.R., Chan, D.W.-H., 2001. Cationic ferritin changes outflow facility in human eyes whereas anionic ferritin does not. Invest. Ophthalmol. Vis. Sci. 42, 1795–1802.

Gills, J.P., Roberts, B.C., Epstein, D.L., 1998. Microtubule disruption leads to cellular contraction in human trabecular meshwork cells. Invest. Ophthalmol. Vis. Sci. 39, 653–658.

Gual, A., Llobet, A., Gilabert, R., Borras, M., Pales, J., Bergamini, M.V., Belmonte, C., 1997. Effects of time of storage, albumin, and osmolality changes on outflow facility (C) of bovine anterior segment in vitro. Invest. Ophthalmol. Vis. Sci. 38, 2165–2171.

Johnson, M., Gong, H., Freddo, T.F., Ritter, N., Kamm, R., 1993. Serum proteins and aqueous outflow facility resistance in bovine eyes. Invest. Ophthalmol. Vis. Sci. 34, 3549–3557.

Johnson, M., Shapiro, A., Ethier, C.R., Kamm, R.D., 1992. Modulation of outflow resistance by the pores of the inner wall endothelium. Invest. Ophthalmol. Vis. Sci. 33, 1670–1675.

Kaufman, P.L., 1992. Pharmacologic trabeculocanalotomy. Facilitating aqueous outflow by assaulting the meshwork cytoskeleton, junctional complexes, and extracellular matrix. Arch. Ophthalmol. 110, 34–36.

Kaufman, P.L., Svedbergh, B., Lütjen-Drecoll, E., 1979. Medical trabeculocanalotomy in monkeys with cytochalasin B or EDTA. Ann. Ophthalmol. 11, 795–796.

Kaufman, P.L., True-Gabelt, B., Erickson-Lamy, K.A., 1988. Time-dependence of perfusion outflow facility in the cynomolgus monkey. Curr. Eye Res. 7, 721–726.

Kee, C., Gabelt, B.T., Gange, S.J., Kaufman, P.L., 1996. Serum effects on aqueous outflow during anterior chamber perfusion in monkeys. Invest. Ophthalmol. Vis. Sci. 37, 1840–1848.

Liu, X., Brandt, C.R., Gabelt, B.T., Bryar, P.J., Smith, M.E., Kaufman, P.L., 1999. Herpes simplex virus mediated gene transfer to primate ocular tissues. Exp. Eye Res. 69, 385–395.

Liu, X., Cai, S., Glasser, A., Volberg, T., Polansky, J.R., Fauss, D.J., Geiger, B., Kaufman, P.L., 2001. Effects of H-7 on cultured human trabecular meshwork cells. Mol. Vis. 7, 145–153. http://www.molvis.org/molvis/v7/a21/.

Maepea, O., Bill, A., 1989. The pressures in the episcleral veins. Schlemm's canal and the trabecular meshwork in monkeys: effects of changes in intraocular pressure. Exp. Eye Res. 49, 645–663.

Mäepea, O., Bill, A., 1992. Pressures in the juxtacanalicular tissue and Schlemm's canal in monkeys. Exp. Eye Res. 54, 879–883.

Overby, D., Gong, H., Qiu, G., Freddo, T., Johnson, M., 2002. The mechanism of increasing outflow facility during washout in the bovine eye. Invest. Ophthalmol. Vis. Sci. 43, 3455–3464.

Sabanay, I., Gabelt, B.T., Tian, B., Kaufman, P.L., Geiger, B., 2000. H-7 effects on structure and fluid conductance of monkey trabecular meshwork. Arch. Ophthalmol. 118, 955–962.

Tian, B., Gabelt, B.T., Peterson, J.A., Kiland, J.A., Kaufman, P.L., 1999. H-7 increases trabecular facility and facility after ciliary muscle disinsertion in monkeys. Invest. Ophthalmol. Vis. Sci. 67, 293–295.

Tian, B., Kaufman, P.L., Volberg, T., Gabelt, B.T., Geiger, B., 1998. H-7 disrupts the actin cytoskeleton and increases outflow facility. Arch. Ophthalmol. 116, 633–643.

Vittitow, J.L., Garg, R., Rowlette, L.L., Epstein, D.L., O'Brien, E.T., Borras, T., 2002. Gene transfer of dominant-negative RhoA increases outflow facility in perfused human anterior segment cultures. Mol. Vis. 8, 32–44.

Volberg, T., Geiger, B., Citi, S., Bershadsky, A.D., 1994. Effect of protein kinase inhibitor H-7 on the contractility, integrity, and membrane anchorage of the microfilament system. Cell Motil. Cytoskeleton 29, 321–338.

Yu, J.C., Gotlieb, A.I., 1992. Disruption of endothelial actin microfilaments by protein kinase C inhibitors. Microvasc. Res. 43, 100–111.